



# Jefferson Lab PAC19 Proposal Cover Sheet

This document must  
be received by close  
of business Thursday,  
Dec. 14, 2000 at:

Jefferson Lab  
User Liaison,  
Mail Stop 12B  
12000 Jefferson Ave.  
Newport News, VA  
23606

Experimental Hall: A  
Days Requested for Approval: 21

Proposal Title:

*A Study of the Dynamics of the  
Exclusive Electro-Disintegration  
of the Deuteron*

### Proposal Physics Goals

Indicate any experiments that have physics goals similar to those in your proposal.

*E84-004, E84-019, E94-102*

Approved, Conditionally Approved, and/or Deferred Experiment(s) or proposals:

### Contact Person

Name: *Werner Boeglin*

Institution: *Florida International University*

Address: *Physics Dept.*

Address:

City, State, ZIP/Country: *Miami, FL 33199*

Phone: *(305) 348 1711*

Fax: *(305) 348 - 6700*

E-Mail: *boeglinw@wanda.fiu.edu*

Jefferson Lab Use Only

Receipt Date: \_\_\_\_\_

By: \_\_\_\_\_

# BEAM REQUIREMENTS LIST

JLab Proposal No.: \_\_\_\_\_ Date: \_\_\_\_\_

Hall: A Anticipated Run Date: \_\_\_\_\_ PAC Approved Days: \_\_\_\_\_

Spokesperson: Werner Boeglin  
 Phone: (305) 348 1711  
 E-mail: boeglinw@fiu.edu

Hall Liaison: \_\_\_\_\_

List all combinations of anticipated targets and beam conditions required to execute the experiment. (This list will form the primary basis for the Radiation Safety Assessment Document (RSAD) calculations that must be performed for each experiment.)

Condition No.	Beam Energy (MeV)	Mean Beam Current ( $\mu$ A)	Polarization and Other Special Requirements (e.g., time structure)	Target Material (use multiple rows for complex targets — e.g., w/windows)	Material Thickness (mg/cm <sup>2</sup> )	Est. Beam-On Time for Cond. No. (hours)
1	4320	100		LD <sub>2</sub>	2400	80
2	5400	100		LD <sub>2</sub>	2400	300
3	4320	50		<sup>12</sup> C	200	40
4	5400	50		<sup>12</sup> C	200	20
5	4320	50		LH <sub>2</sub>	1000	10
6	5400	50		LH <sub>2</sub>	1000	10

The beam energies,  $E_{\text{Beam}}$ , available are:  $E_{\text{Beam}} = N \times E_{\text{Linac}}$  where  $N = 1, 2, 3, 4, \text{ or } 5$ .  $E_{\text{Linac}} = 800$  MeV, i.e., available  $E_{\text{Beam}}$  are 800, 1600, 2400, 3200, and 4000 MeV. Other energies should be arranged with the Hall Leader before listing.

# HAZARD IDENTIFICATION CHECKLIST

JLab Proposal No.: \_\_\_\_\_

Date: \_\_\_\_\_

(For CEBAF User Liaison Office use only.)

Check all items for which there is an anticipated need.

<p><b>Cryogenics</b></p> <p>_____ beamline magnets</p> <p>_____ analysis magnets</p> <p><input checked="" type="checkbox"/> target</p> <p>type: _____</p> <p>flow rate: _____</p> <p>capacity: _____</p>	<p><b>Electrical Equipment</b></p> <p>_____ cryo/electrical devices</p> <p>_____ capacitor banks</p> <p>_____ high voltage</p> <p>_____ exposed equipment</p>	<p><b>Radioactive/Hazardous Materials</b></p> <p>List any radioactive or hazardous/toxic materials planned for use:</p> <p>_____</p> <p>_____</p> <p>_____</p>
<p><b>Pressure Vessels</b></p> <p>_____ inside diameter</p> <p>_____ operating pressure</p> <p>_____ window material</p> <p>_____ window thickness</p>	<p><b>Flammable Gas or Liquids</b></p> <p>type: <u>LH<sub>2</sub>/LDe</u></p> <p>flow rate: _____</p> <p>capacity: _____</p> <p><b>Drift Chambers</b></p> <p>type: _____</p> <p>flow rate: _____</p> <p>capacity: _____</p>	<p><b>Other Target Materials</b></p> <p>_____ Beryllium (Be)</p> <p>_____ Lithium (Li)</p> <p>_____ Mercury (Hg)</p> <p>_____ Lead (Pb)</p> <p>_____ Tungsten (W)</p> <p>_____ Uranium (U)</p> <p>_____ Other (list below)</p> <p>_____</p> <p>_____</p>
<p><b>Vacuum Vessels</b></p> <p>_____ inside diameter</p> <p>_____ operating pressure</p> <p>_____ window material</p> <p>_____ window thickness</p>	<p><b>Radioactive Sources</b></p> <p>_____ permanent installation</p> <p>_____ temporary use</p> <p>type: _____</p> <p>strength: _____</p>	<p><b>Large Mech. Structure/System</b></p> <p>_____ lifting devices</p> <p>_____ motion controllers</p> <p>_____ scaffolding or</p> <p>_____ elevated platforms</p>
<p><b>Lasers</b></p> <p>type: _____</p> <p>wattage: _____</p> <p>class: _____</p> <p><b>Installation:</b></p> <p>_____ permanent</p> <p>_____ temporary</p> <p><b>Use:</b></p> <p>_____ calibration</p> <p>_____ alignment</p>	<p><b>Hazardous Materials</b></p> <p>_____ cyanide plating materials</p> <p>_____ scintillation oil (from)</p> <p>_____ PCBs</p> <p>_____ methane</p> <p>_____ TMAE</p> <p>_____ TEA</p> <p>_____ photographic developers</p> <p>_____ other (list below)</p> <p>_____</p> <p>_____</p>	<p><b>General:</b></p> <p><b>Experiment Class:</b></p> <p>_____ Base Equipment</p> <p>_____ Temp. Mod. to Base Equip.</p> <p>_____ Permanent Mod. to</p> <p>_____ Base Equipment</p> <p>_____ Major New Apparatus</p> <p><b>Other:</b> _____</p> <p>_____</p>

# Computing Requirements List

Proposal Title: A Study of the Dynamics of the Exclusive Electro-Disintegration of the Deuteron

Spokesperson: W. Boeglin Experimental Hall: A

## Raw Data Expected

Total: 2Tb Per Year (long duration experiments only): \_\_\_\_\_

Simulation Compute Power (SPECint95 hours) Required: \_\_\_\_\_

On-Line Disk Storage Required: 100 Gb

Imported Data Amount from Outside Institutions: \_\_\_\_\_

Exported Data Amount to Outside Institutions: 300 Gb

Expected Mechanism for Imported/Exported Data: FTP/SSH, tapes

## Special Requirements

For example, special configuration of data acquisition systems) that may require resources and/or coordination with JLab's Computer Center. Please indicate, if possible, what fraction of these resources will be provided by collaborating institutions and how much is expected to be provided by JLab.

---

---

---

---

---

---

---

---

---

---

# LAB RESOURCES LIST

JLab Proposal No.: \_\_\_\_\_

*(For JLab ULO use only.)*

Date \_\_\_\_\_

List below significant resources — both equipment and human — that you are requesting from Jefferson Lab in support of mounting and executing the proposed experiment. Do not include items that will be routinely supplied to all running experiments such as the base equipment for the hall and technical support for routine operation, installation, and maintenance.

**Major Installations** *(either your equip. or new equip. requested from JLab)*

---

---

---

---

---

*New Support Structures:* \_\_\_\_\_

---

---

---

**Data Acquisition/Reduction**

*Computing Resources:* \_\_\_\_\_

---

---

---

*New Software:* \_\_\_\_\_

---

---

---

**Major Equipment**

Magnets: \_\_\_\_\_

---

Power Supplies: \_\_\_\_\_

---

Targets: \_\_\_\_\_

---

Detectors: \_\_\_\_\_

---

Electronics: \_\_\_\_\_

---

Computer Hardware: \_\_\_\_\_

---

Other: \_\_\_\_\_

---

**Other:** \_\_\_\_\_

---

---

---

# A Study of the Dynamics of the Exclusive Electro-Disintegration of the Deuteron

W. Boeglin (*Spokesperson*), F. Klein, L. Kramer, P. Markowitz, B. Raue, J. Reinhold,  
M. Sargsian

*Florida International University*

A. Klein (*Co-Spokesperson*), S. Kuhn, L.B. Weinstein

*Old Dominion University*

G. Batigne, C. Furget, S. Kox, E. Liatard, J. Mougey, E. Penel, J.-S. Réal, R. Tieulent,  
E. Voutier (*Co-Spokesperson*)

*Institut des Sciences Nucléaires, Grenoble*

S. Jeschonnek

*Jefferson Lab*

W. Bertozzi, S. Gilad, D.W. Higinbotham, M. Ryachev, S. Sirca, R. Suleiman, Z. Zhou

*Massachusetts Institute of Technology*

E. Piasetzky

*Tel Aviv University*

M. Strikman

*Pennsylvania State University*

J. Templon

*University of Georgia*

J.-M. Laget

*Centre d'Etudes de Saclay, Gif-sur-Yvette*

Hall A Collaboration

December 14, 2000

## Abstract

This proposal aims at a quantitative study of the dynamics of Final State Interactions, Meson Exchange Currents and Isobaric Currents in the electro-disintegration of the deuteron in order to investigate the short range structure of this few body system. The  $D(e,e'p)n$  reaction will be studied by measuring the coincidence cross section for  $Q^2$  -values of 1.0, 2.5, and 4.0  $(\text{GeV}/c)^2$  and recoil momenta values ( $p_{miss}$ ) between 0.2 and 0.5  $\text{GeV}/c$ . A complete angular distribution of the recoiling neutron with respect to the virtual photon will be obtained for each combination of fixed  $p_{miss}$  and  $Q^2$ .

# 1 Introduction

The understanding of the short-range structure of the bound two-nucleon system - the deuteron, is of fundamental importance for the advancement of the theory of nuclear matter at short distances. To probe the short-range properties of the deuteron one has to investigate configurations where the two nucleons come very close together and are essentially strongly overlapping. The basic problem is to what extent these configurations can be described in terms of two nucleons with high initial relative momenta (Fermi momenta). Traditionally three classes of reactions are used to study the high momentum part of the deuteron wave function: elastic scattering, inclusive and exclusive electro-disintegration reactions.

Elastic electron-deuteron scattering at large transferred 4-momentum  $Q^2$ , being sensitive to the high momentum component of the deuteron wave function, probes the integrated characteristics of the wave function via the deuteron form-factors. The analysis of the recent experimental data [1] showed that, at presently available energies, it is practically impossible to discriminate between different theoretical approaches [2] used to calculate the deuteron elastic form-factor  $A(Q^2)$ . The main problem is the lack of an independent determination of the deuteron wave function at large nucleon momenta (i.e. short distances).

Inclusive, inelastic ( $e, e'$ ) reactions provide a more direct way of probing high momentum components of the deuteron especially at high  $Q^2$  and in the  $x \geq 1$  regime [3]. In this regime the measured cross section is sensitive to the longitudinal component of the deuteron momentum distribution with respect to the virtual photon momentum  $\vec{q}'$ . However the impossibility to isolate inelastic (nucleon) contributions (growing with  $Q^2$ ) and final state interactions at large  $x$  (see e.g. [4, 5, 6]), preclude a direct access to the deuteron wave function at short inter-nucleon distances (although the high-momentum component is certainly important in this kinematics).

The most direct way of studying high nucleon momenta is to investigate the quasi-elastic electro-disintegration of the deuteron via the  $D(e, e'p)n$  reaction at high missing momenta  $p_{miss}$ . Within the Plane Wave Impulse Approximation (PWIA)  $p_{miss}$  corresponds to the initial momentum of the target nucleon before the interaction. Thus the strategy in these studies is to probe the cross section at  $p_{miss}$  values as large as possible. However, depending on the selected kinematics, these studies can be overwhelmed by inelastic (meson and  $\Delta$ -isobar) channels. This has been confirmed by early experiments at low/intermediate energies of scattered electrons [7]. Also more recent experiments [8] at slightly higher energies and momentum transfers found that in the regime of large  $p_{miss}$  medium/long range (soft) two-body currents such as meson-exchange currents and isobar contributions significantly dominate the cross section. In general, to suppress processes due to large inter-nucleon distances and to enhance contributions of reaction mechanisms which probe the short-distance structure of the deuteron, *the transferred momentum in the reaction should typically be larger than 1 GeV/c*.

This experiment proposes to measure the coincidence cross section for the electro-disintegration of the deuteron

$$e + d \rightarrow e' + p + n \tag{1}$$

at four momentum transfers of  $Q^2 = 1.0, 2.5$  and  $4.0$  (GeV/c)<sup>2</sup> and missing momenta of

$p_{miss} = 0.2, 0.4$  and  $0.5$  GeV/c. These measurements will be carried out in quasi-elastic kinematics for which we use the notations:  $q=(q_0, \vec{q})$  for the 4-momentum of the virtual photon ( $Q^2 = q^2 - q_0^2$ ), and  $p_d=(m_d, \vec{0})$  and  $p_f=(E_f, \vec{p}_f)$  for the target deuteron and the detected nucleon 4-momenta respectively. For each value of  $Q^2$  and  $p_{miss}$  the angle of the recoiling neutron, with respect to the momentum transfer, will be varied to build a complete angular distribution of the differential cross section over the full available phase space. As shown in the following sections, this will provide the necessary experimental information on the D(e,e'p)n reaction at high  $Q^2$ , covering both  $x < 1$  and  $x > 1$  regions, to allow us to address the problems of:

- the Final State Interactions (FSI) between knock-out and recoil nucleon,
- the Meson-exchange Currents (MEC) and Isobar Current (IC) contributions,
- and the dynamics of the bound two nucleon system.

*The quantitative understanding of these processes is the inescapable preliminary step towards the study of the Short Range NN Correlations (SRC) in the deuteron and the eventual manifestation of non-nucleonic/quark-gluon degrees of freedom in this nucleus.*

## 2 Physics Motivations

A comprehensive program of experimental studies of high  $Q^2$  electro-disintegration of the deuteron will have a significant impact on our understanding of the structure of the  $NN$  interaction at short-distances. Measurements of the D(e,e'p)n cross section in a wide range of missing momenta, recoil nucleon angles, and the virtuality of the exchanged photon will allow us to eventually disentangle the different processes contributing to this reaction that are currently discussed in the literature.

### 2.1 Final State Interactions

Within PWIA, the out-going nucleon does not interact with the residual system after the interaction with the virtual photon. However in the kinematic region where one expects to have an enhanced contribution from SRC one may also expect a substantial contribution from FSI between the knock-out and the spectator nucleon. The main effect introduced by FSI is that the nucleon momentum (say  $\tilde{p}_{miss}$ ), carried by the bound nucleon before the interaction with the electron, is not the same as the one measured in the experiment  $\vec{p}_{miss} = \vec{p}_f - \vec{q}$ . As a result one can not be confident that the condition of large  $p_{miss}$ , automatically guarantees that high momentum components in the ground state wave function of the deuteron are measured. In all previous D(e,e'p)n experiments at large  $p_{miss}$  the FSI were a major contributor to the overall cross section and therefore substantially overshadowed SRC.

With increasing energies, the situation changes qualitatively. At large angular momenta, FSI are dominated by the  $pn$  re-scattering and then become strongly anisotropic with respect

to the direction of  $\vec{q}$ . The maximal re-scattering happens in directions almost transverse to  $\vec{q}$ . Consequently, FSI contribute much less for parallel and anti-parallel kinematics and can be treated there as a correction. *However this phenomenon has still to be observed experimentally for the  $D(e,e'p)n$  reaction.*

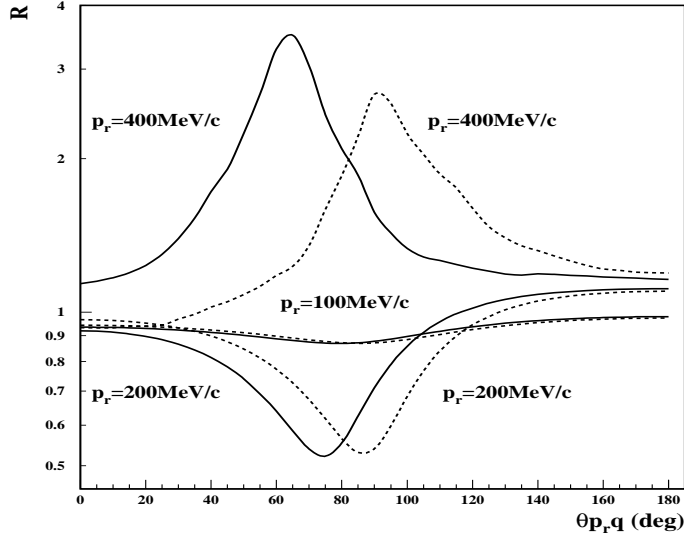


Figure 1: The angular dependence of  $R$ , the ratio of the  $D(e,e'p)n$  cross section calculated including PWIA and FSI terms to the cross section which includes PWIA term only: GEA (solid line) and according to the conventional Glauber approximation (dashed line).

The dominance of large angular momenta allows to apply eikonal approximations in calculating FSI. A well known example of the eikonal approximation of FSI is the Glauber approximation [9]. However the latter was derived for cases where one can neglect the motion of bound nucleons in the nucleus. For the  $D(e,e'p)n$  reaction at large missing momenta, the eikonal approximation was generalized (GEA) in order to account for finite values of nucleon momenta [10, 11]. Fig. 1 represents the ratios of the calculated cross sections that include FSI to the one within PWIA only. The ratios are shown for different values of recoil momenta as a function of the angle between the recoiling nucleon and  $\vec{q}$ . The calculations here are carried out within the conventional Glauber approximation and the generalized Glauber approximation (GEA). It is shown that while being similar at small values of  $p_{miss}$  the predictions substantially diverge at larger  $p_{miss}$  values.

The eikonal approximation is expected to become decreasingly valid for smaller energies. Indeed, when the center of mass energy of the final  $pn$  system decreases, the relative momenta in the  $pn$  system become small and the eikonal approximation should break down to let place to an intermediate energy regime. However, it is not clear at which  $Q^2$ -value the transition between these two regimes takes place. Data from an experiment on nucleon propagation in the  $A(e,e'p)X$  reaction [12, 13] indicates that this transition happens already at  $1 \text{ (GeV/c)}^2$ . However these data are taken for small values of  $p_{miss} \leq 200 \text{ MeV/c}$  and it is quite likely that this transition depends on  $p_{miss}$ , especially for the  $x \geq 1$  kinematics ( $\theta_{p,q} < 90^\circ$  in Fig. 1). A comparison [10] of calculations carried out within the medium energy approach [14], in

which the  $pn$  final state was calculated by summing all states with angular momenta  $l \leq 7$ , and the GEA, indicates that for the case of larger  $p_{miss}$  the transition happens already at  $Q^2 \approx 1$  (GeV/c)<sup>2</sup>. This is confirmed by the diagrammatic approach of Laget [15], which deals with interaction effects (FSI, MEC, IC) without kinematical approximations. The kinematics is relativistic, and the full angular dependency of the elementary operator is kept in the loop integrals. Only positive energy components of the wave functions are retained, and are parametrized by solution of the Lippman-Schwinger equation for the Paris Potential (the argument of the bound state wave function is the relativistic momentum of the spectator nucleon). The elementary electromagnetic operator is expanded in power of  $p/m$ , up to and including term in  $(p/m)^4$  [16]. Instead of the partial expansion of the nucleon-nucleon scattering amplitude [15, 16], the model is extended to high energy by parameterizing the scattering amplitude as  $\propto \sigma_{NN} \exp(bt)$ , with the experimental values of  $\sigma_{NN}$  and  $b$  [17, 18]. Fig. 2 shows that the peak in the FSI occurs at the same place as in the GEA treatment. It is a straight forward consequence of unitarity, as its maximum occurs when on-shell scattering is maximized in the FSI loop integral at  $x = Q^2/2m\nu = 1$ .

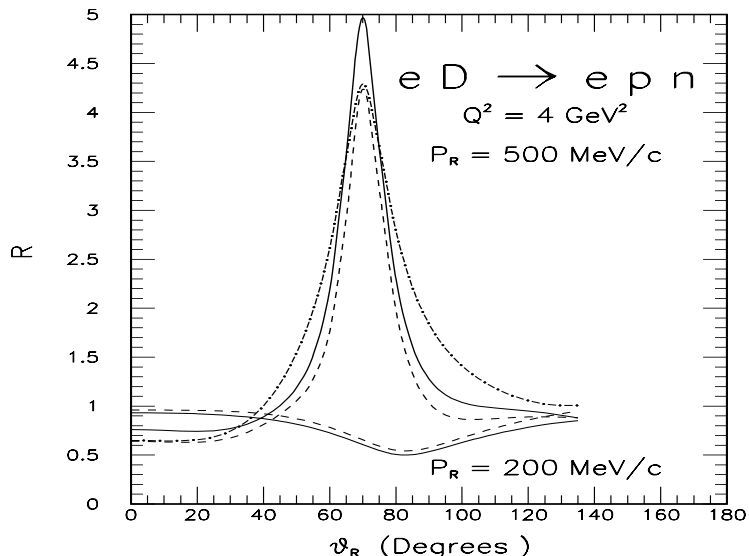


Figure 2: The angular dependence of the ratio of the  $D(e,e'p)n$  cross section calculated within different approaches to the cross section including PWIA term only: factorized PWIA+FSI (solid lines) and unfactorized PWIA+FSI (dashed lines).

Finally, a measurement of the  $D(e,e'p)n$  cross section as a function of the angle of the recoiling nucleon will indicate those regions where FSI can be factorized from the initial  $\gamma^*N$  interaction. These regions are very important for isolating the physics related to the  $\gamma^*N$  interaction (EMC type phenomena) from the one related to the physics of the  $NN$  interaction at large  $Q^2 \geq 4$  (GeV/c)<sup>2</sup> (Color Transparency). An advantage of the deuteron is that unfactorized calculations can be realized in a straightforward way depending upon certain assumptions on the structure of  $NN$  interaction. One such calculation based on the conventional Glauber approximation [19] has been carried out in Ref. [20]. A quantitative estimate of the effects of factorization has been performed in the framework of Laget's

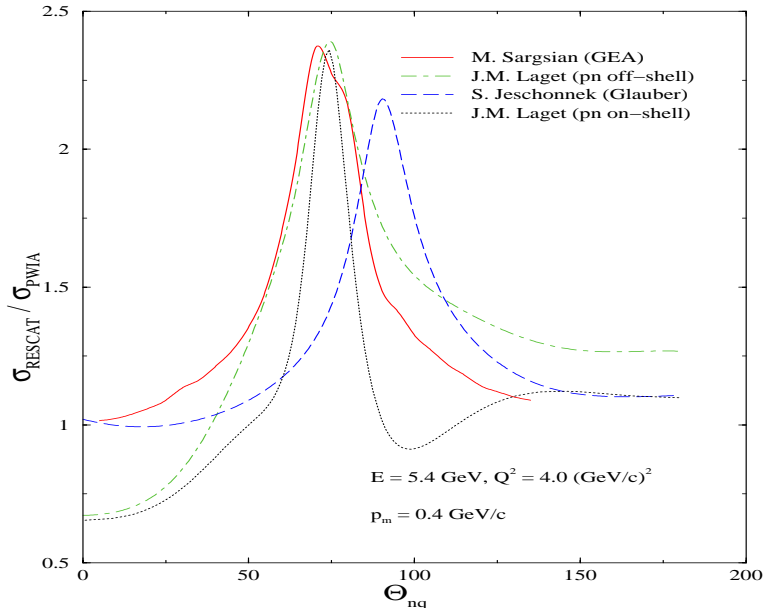


Figure 3: The ratio between the  $D(e,e'p)n$  cross section calculated including FSI and PWIA for  $Q^2 = 4 \text{ (GeV/c)}^2$  and  $p_{\text{miss}} = 0.4 \text{ GeV/c}$ .

approach. As demonstrated in Fig. 2, they are not important and do not alter significantly the shape and the magnitude of the rescattering peak. On the other hand, the scattered proton can be off-shell. Contrary to the on-shell part, this part of the rescattering amplitude is model dependent, since it depends on the half-off-shell  $pn$  scattering amplitude which is poorly known in the GeV energy range. However, as can be seen in Fig. 2 the off-shell rescattering contribution does not affect the height of the FSI peak (it vanishes here), while it slightly broadens its tails. Fig. 3 compares the three different approaches. When off-shell  $pn$  rescattering is allowed, the Laget approach is very similar to the GEA. In the following only the iron clad on-shell rescattering has been retained in Laget's approach. The measurements of the  $D(e,e'p)n$  cross section at  $p_{\text{miss}} \geq 0.4 \text{ GeV/c}$  will be able to provide important new information about these issues.

This experiment proposes to address these problems by measuring, for several  $Q^2$  and recoil angles, a ratio like

$$R(Q^2, \theta_{p,q}) = \frac{\sigma(p_m = 0.2, 0.4, 0.5)}{\sigma(p_m^{\text{ref.}} = 0.05)} \quad (2)$$

which is the ratio of the cross section at given  $p_{\text{miss}}$  to the cross section at a small reference missing momentum for which the PWIA is valid. The study of the  $\theta_{p,q}$  dependence of such a ratio at fixed  $Q^2$  will allow to isolate FSI effects and investigate the factorization of the FSI and the  $\gamma^*N$  interaction. An important goal of these measurements will be to confirm the theoretical expectation that FSI are generally suppressed in parallel and anti-parallel kinematics compared to perpendicular kinematics. The experimental verification of this prediction is very important since it might open a window to directly probe contributions of SRC to the nucleons wave function.

## 2.2 Meson Exchange Currents and Isobar Contributions

Experimental  $D(e,e'p)n$  data at low  $Q^2$  demonstrated that with increasing  $p_{miss}$  MEC and IC become dominant, making it virtually impossible to extract information on short-range  $NN$  correlations. The calculation of MEC and IC at high  $Q^2$  is very complicated since the

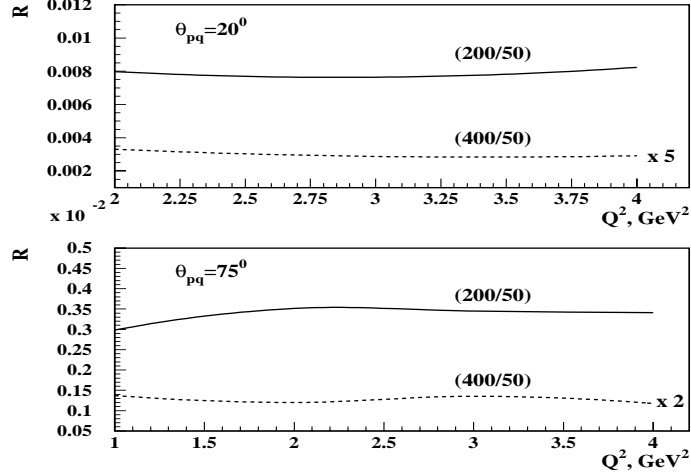


Figure 4:  $Q^2$  dependence of the ratio  $R$  (Eq. 2) for  $p_{miss} = 0.2-0.4$  GeV/c and  $\theta_{pq} = 20-70^\circ$ .

virtuality of the exchanged mesons greatly exceeds their masses. However it is possible to estimate the  $Q^2$  -dependence of these contributions based on the analysis of the corresponding Feynman diagrams. Theoretically one expects that the MEC contribution will decrease with increasing  $Q^2$ . Indeed it can be shown that MEC diagrams have an additional  $\sim 1/Q^2$  dependence compared to the diagrams where the electron scatters from a nucleon. This suppression comes from two major factors. Firstly, because at the considered kinematics the knocked-out nucleon is fast and takes almost the entire momentum of the virtual photon  $q$ , the exchanged meson propagator is proportional to  $(1 + Q^2/m_{meson}^2)$ . Secondly, an additional  $Q^2$  dependence comes from the  $NN - meson$  form-factor  $\sim (1 + Q^2/\Lambda^2)$ . Thus the overall additional dependence as compared to PWIA diagram is [21]

$$\frac{1}{(Q^2 + m_{meson}^2)} \Gamma_{MNN}(Q^2) \propto \left( \frac{1}{(Q^2 + m_{meson}^2)} \frac{1}{(1 + Q^2/\Lambda^2)^2} \right) \quad (3)$$

where  $m_{meson} \approx 0.71$  and  $\Lambda^2 \sim 0.8-1$  (GeV/c)<sup>2</sup> <sup>1</sup>. Thus one expects that MEC contributions will be strongly suppressed as soon as  $Q^2 \geq m_{meson}^2$  and  $\Lambda \sim 1$  (GeV/c)<sup>2</sup>. As can be seen in Fig. 4 the  $Q^2$  dependence of the ratio  $R$  (Eq. 2) including FSI is very weak. This is confirmed by another estimate performed in Laget's approach (Fig. 5). At low  $Q^2$ , MEC and IC contribution is not negligible, as the invariant mass of the  $np$  system spans the baryonic resonance regime. Their contribution is clearly suppressed at higher  $Q^2$ . Note also

<sup>1</sup>We assume here that different meson-nucleon vertices have a similar dependence on  $Q^2$ . Assuming the dipole dependence on  $Q^2$  corresponds to neglecting the size of a meson as compared to the size of a baryon (for large  $Q^2$  quark counting rules lead to  $\Gamma_{MNN}(Q^2) \sim \frac{1}{Q^6}$ ). We also use restrictions on the  $Q^2$  -dependence of the  $\pi NN$  vertex from measurements of the antiquark distribution in nucleons [22].

that the MEC seem to be enhanced in the region of  $\theta_{p,q} > 90^\circ$  which is covered by the proposed experiment. This is the region which is closely connected to the kinematics of the large angle  $\gamma + D \rightarrow pn$  experiment where the MEC picture seems to break down at  $Q^2$  values  $\sim 1 \text{ (GeV/c)}^2$ . In addition, the MEC contribution in the region of maximum FSI is shown to be small, making the projected measurement of FSI increasingly reliable.

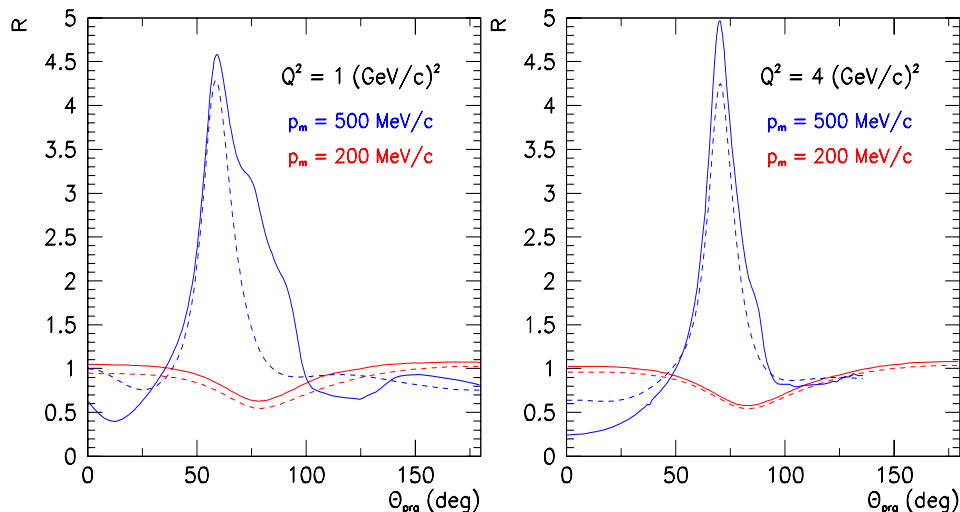


Figure 5: The angular dependence of  $R$ , the ratio of the  $D(e,e'p)n$  cross section calculated within different approaches to the cross section including PWIA term only: PWIA+FSI only (dashed curves), PWIA+FSI+MEC+IC (full curves).

Hence getting complementary data sensitive to MEC effects for large momentum transfers is very interesting. One may expect that in the long run such measurements would permit to discriminate between meson exchange [23] and quark exchange pictures [24] of large angle emission of nucleon pairs. To estimate the IC contribution, we observe that the  $x < 1$  and  $x > 1$  regions at the same  $p_{miss}$  have different contributions from intermediate  $\Delta$  excitations. In this case the amplitude of the IC contribution is proportional to:

$$\psi_D \left( p_{mt}, p_{mz} - \frac{M_\Delta^2 - M_N^2}{2q} \right), \quad (4)$$

where  $p_{mt}$  and  $p_{mz}$  are the transverse and longitudinal components of the measured missing momentum. This equation shows that one can expect more IC contributions in the  $x < 1$  region than in the  $x > 1$  since in that case  $p_{mz} - \frac{M_\Delta^2 - M_N^2}{2q} < p_{mz}$ . Thus a combined study of the cross section at constant  $p_{miss}$  but different  $x$  regions will be sensitive to IC contributions in the overall cross section.

### 2.3 The Dynamics of Deeply Bound Nucleons

Once the contributions due to SRC are isolated, by deconvoluting from FSI+MEC+IC contributions, the fundamental question that remains is the dynamics of the electromagnetic interaction of deeply bound nucleons in SRC. The investigation of the cross section in near

parallel  $x < 1$  and anti-parallel  $x > 1$  kinematics, where FSI are expected to be a correction, as discussed above, will yield important information about the structure of vacuum fluctuations. The problem here is that, with increasing missing momentum in nuclei the relative contribution of vacuum diagrams also increases. By vacuum diagrams one means the process where the virtual photon splits into a  $N\bar{N}$  pair (Fig. 6). The  $\bar{N}$  is subsequently absorbed by the nucleus, yielding the same final hadronic state, that the direct knock-out process would have produced. To solve this known theoretical problem, a number of theoretical prescrip-

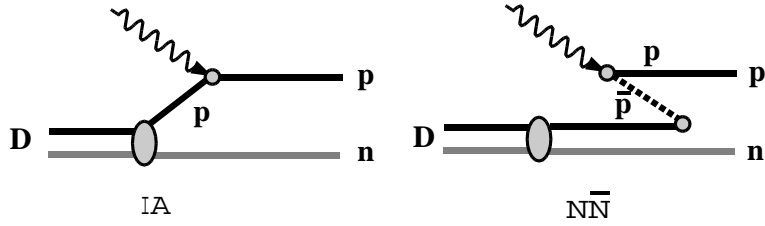


Figure 6: Impulse approximation (IA) and vacuum diagrams ( $N\bar{N}$ ) diagrams for the electrodisintegration of the deuteron

tions have been developed [25, 26]. One of the methods is the development of the Light Cone (LC) dynamics of nuclei, where the contribution of vacuum diagrams are effectively calculated in the LC reference frame [25]. As a result in this case (similar to the high energy scattering in QCD) the LC nuclear wave function of the nucleus which emerges [25, 27, 28], depends on the variables  $p_{m+}/p_D^+ \equiv \alpha$  and  $p_{mt}$ . In the approximation when the deuteron is described as a two nucleon system there is an unambiguous connection between the LC and the non-relativistic wave function. In this case the LC wave function essentially depends only on the invariant mass of the two-nucleon system [25]. If mesonic degrees of freedom are included in the deuteron wave function, it depends on the two independent variables  $\alpha$ , and  $p_{mt}$ , and can be explicitly calculated within particular models (see e.g. [29]). The overall cross section of the  $D(e,e'p)n$  reaction is then the convolution of the off- $p_{m-}$ -shell  $\gamma^*N$  cross section and the LC deuteron wave function. Another description of the deeply bound nucleon is the virtual nucleon approximation [30], where the virtuality of the nucleon has been introduced while in the laboratory frame. In this case the PWIA cross section is expressed through a non-relativistic deuteron wave function and an off-energy( $E_m$ )-shell  $\gamma^*N$  cross section. In the Laget's approach, an expansion in power of  $p/m$  is used, and no LC correction is made on the argument of the nuclear wave function. Up to  $Q^2 \simeq 2.5$  (GeV/c)<sup>2</sup>, this prescription is similar to the popular de Forest's one but it differs above. Today, there are many different approaches on how to treat the interaction of an electron with a bound nucleon at large  $Q^2$ . *A dedicated measurement is mandatory to provide us with a guide in this matter.* Fig. 7 compares the cross sections calculated with the LC and virtual nucleon approximations. It shows that for small recoil angles the two approaches predict very similar cross sections. This should therefore allow us to directly measure the deuteron wave function. As an example Fig. 8 shows cross sections calculated using wave functions based on the Paris and the Bonn potentials. It is very important that these comparisons will be done at fixed values of  $Q^2$  which will enable us to isolate the effects related to the modi-

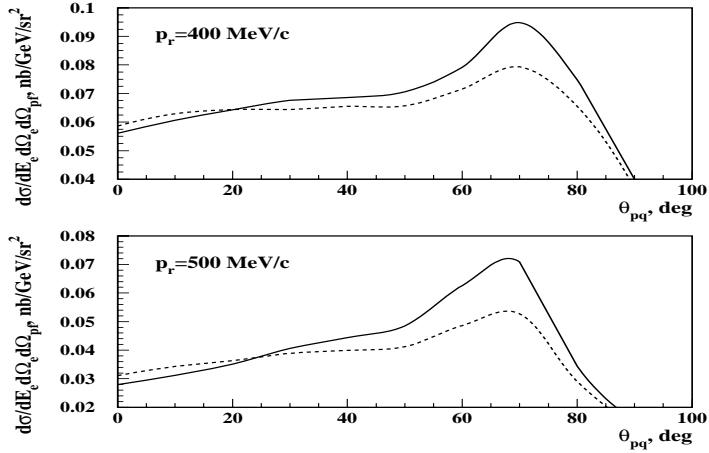


Figure 7: Angular dependence of the  $D(e,e'p)n$  cross section calculated with the virtual nucleon (solid line) and the light cone (dashed line) approximations for  $Q^2 = 4.0$   $(\text{GeV}/c)^2$

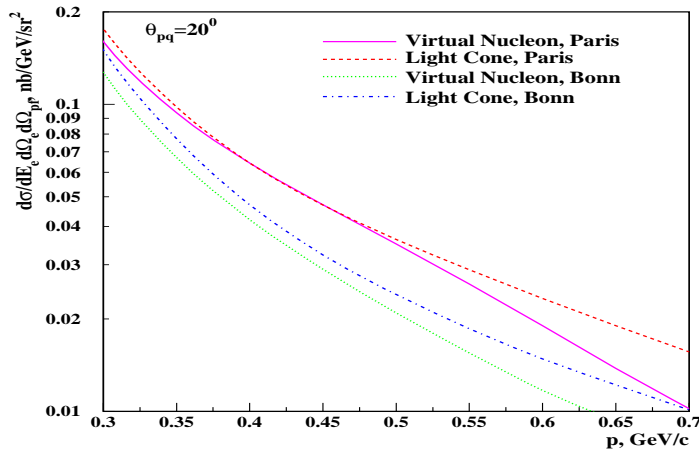


Figure 8: The  $D(e,e'p)n$  cross section for  $\theta_{pq} = 20^\circ$  calculated within the virtual nucleon and the light cone approach.

fication of the deeply bound nucleon's quark-gluon wave function (similar as in EMC-type effects). The  $p_{miss}$  dependence of the ratio of the  $D(e,e'p)n$  cross section in parallel ( $x > 1$ ) and anti-parallel ( $x < 1$ ) kinematics measured at lower and higher values of  $Q^2$  will test the form-factor modification of deeply bound nucleons.

### 3 A Look Into the Future

*Upon the quantitative understanding of the role of FSI, MEC, and IC in the electro-disintegration of the deuteron, one can start to address the important question of quark-gluon degrees of freedom in the deuteron.*

The following projects may be part of a future experimental program, however, the proposed experiment might allow us first glimpses of these physics issues.

### 3.1 Onset of Quark-Gluon Degrees of Freedom

Upon verification of the smallness of FSI in (near) parallel and anti-parallel kinematics, the measurements of the cross section at larger values of  $p_{miss}$  (up to 700 MeV/c), where one expects that the two nucleon picture of the nucleon may still be valid, allows to study the nature of the core of the  $NN$  interaction. It is well known that the wave function of the deuteron diverges substantially in the region where the large repulsion of the  $NN$  interaction becomes important when calculated using different parameterizations of the  $NN$  potential. One of the reasons for this is that the current models do not fit phase-shifts in the region  $T_N \geq 300$  MeV where meson production is allowed and which is very important for the calculation of the deuteron wave function for  $k \geq 0.5$  GeV/c.

The high  $Q^2$  domain and the  $x > 1$  region allow to explore the very large missing momenta region where we expect that the nucleonic picture of the deuteron will break down. The onset of quark degrees of freedom will be dominated by quark-interchange mechanisms in short range interactions. Although it is impossible at this point to predict the absolute values of such contributions, the scenario for a different number of quark exchanges will provide different deuteron momentum distributions.

Extending the cross section measurement to the region of high and very high missing momentum ( $p_{miss} > 700$  MeV/c) will allow to reach the region where quark-exchange diagrams play a dominant role in SRC in the deuteron.

### 3.2 Quark-Gluon Structure of Deeply Bound Nucleons

Experiments of inclusive Deep Inelastic (DIS) electron scattering from nuclei demonstrated the modification of the nucleon quark-parton density as compared to that of the free nucleon (the EMC effect [31]). This effect unambiguously demonstrated that nuclei can not be described merely as a collection of unmodified nucleons. Moreover the proportionality of the EMC effect to the nuclear density was an indication that the modification of the quark-parton structure of nucleons depends on how strong nucleons are bound in a nucleus. Although the effect is observed in the DIS region, one should expect a similar modification for the elastic form-factors of bound nucleons. However, inclusive data alone will not allow one to conclusively check the existence of EMC type phenomena for the elastic form factors. One problem is that with the increase of  $Q^2$ , inelastic channels dominate the inclusive cross section and are thus obscuring elastic contributions [6].

One mechanism of the bound nucleon's form-factor modification is described in the color screening model [32, 33], where at sufficiently high values of  $Q^2 \geq Q_0^2$  ( $Q_0^2 \approx 2-3$  (GeV/c)<sup>2</sup>) the nucleon form-factor becomes sensitive to quark correlations. In this regime the bound nucleon will have suppressed quark correlations as compared to the free nucleon. The reason of such a suppression is the color-screening between quark-correlations which tends to minimize the nuclear binding. In this model the bound nucleon form-factor in the regime of scattering off a small size configuration is suppressed by a factor  $f$ :

$$f = 1 / \left[ 1 + \frac{(k^2 + m_N \epsilon_D)}{m_N \Delta E} \right]^2 \quad (5)$$

where  $\Delta E \sim m_{N^*} - m_N \sim 600$  MeV and  $k$  is the spectator momentum. This factor strongly depends on  $k$  and hence could be tested in the discussed process. Note here that some indications of such an effect were found [34] in the  $x > 1$ ,  $Q^2 \geq 4$  (GeV/c)<sup>2</sup> kinematics for the SLAC  $x > 1$  data. In parallel and anti-parallel kinematics where FSI are small, one can search for the possible bound nucleon modifications, by measuring the  $p_{miss}$  dependence of the ratio of two D(e,e'p)n cross sections measured at the same  $\vec{p}_m$  but different values of  $Q^2$  ( $Q_2^2 \geq Q_0^2$  and  $Q_1^2 \leq Q_0^2$ ).

## 4 Experimental Program

As a first step into the investigation of the D(e,e'p)n reaction at large values of  $Q^2$  we will measure the D(e,e'p)n cross section at the following values for  $Q^2$  : 1.0, 2.5 and 4.0 (GeV/c)<sup>2</sup>. At each momentum transfer the D(e,e'p)n cross section will be measured for the recoil momenta  $p_{miss} = 0.2, 0.4$  and  $0.5$  GeV/c. Keeping the recoil momentum constant, the angle of the recoiling neutron with respect to  $\vec{q}$  will be varied. For  $p_{miss} = 0.2$  GeV/c and  $p_{miss} = 0.4$  GeV/c the recoil angle will be varied between in the domains  $20^\circ - 150^\circ$  and  $20^\circ - 110^\circ$  respectively. This corresponds to a variation in x-Bjorken between typically 0.7 and 1.5. This variation of the neutron angle allows us to study in detail the effect of final state interactions as has been outlined in the previous sections. Small recoil momentum of the order of 50 MeV/c will be measured as a normalization measurement since at these values contributions of FSI, MEC and IC are small. This has been confirmed by measurements at much lower  $Q^2$  values [8, 12, 35].

As can be seen in Fig. 9 at  $p_{miss} = 0.2$  GeV/c, FSI reduce the cross section by approximately a factor of two at a neutron angle around  $70^\circ$  while at  $p_{miss} = 0.4$  GeV/c the cross section is enhanced by a factor of about 2.5 and even larger at higher missing momenta. It is the goal of this experiment to measure this behavior qualitatively and quantitatively for various  $Q^2$  -values. We will measure the cross section in a bin of missing momentum of  $\pm 20$  MeV/c and in a bin of  $\theta_{nq} = \pm 5^\circ$  for the recoil angle (the angle between the recoiling neutron and the momentum transfer) with an expected statistical precision of 5 %. In the region of the large cross section enhancement, data will be taken in  $\theta_{nq}$ -steps of  $10^\circ$ . This should permit us to extract the location and the strength of this structure for various momentum transfers.

Fig. 10, 11 and 12 show the calculated cross sections with and without FSI effects. The points with error bars indicate the projected experimental data including statistical errors. Since no previous experiment has been carried out in these regimes the figures also show the projected data if PWIA were valid. For both projections the same amount of beam time has been assumed. It is important to note that at the lowest  $Q^2$  value of 1.0 (GeV/c)<sup>2</sup> the eikonal approach is not expected to be valid for neutron angles below  $60^\circ$  and missing momenta of 0.2 GeV/c, 0.4 GeV/c, and 0.5 GeV/c, since the proton momenta are still well below 1 GeV/c in these cases. This limit has been marked with a dashed vertical line on each relevant graph.

The measurements at  $p_{miss} = 0.5$  GeV/c are of a more exploratory nature. The effects due to FSI in perpendicular kinematics are predicted to be even larger than for 0.4 GeV/c.

Due to the reduced cross section we will therefore measure those with a statistical precision

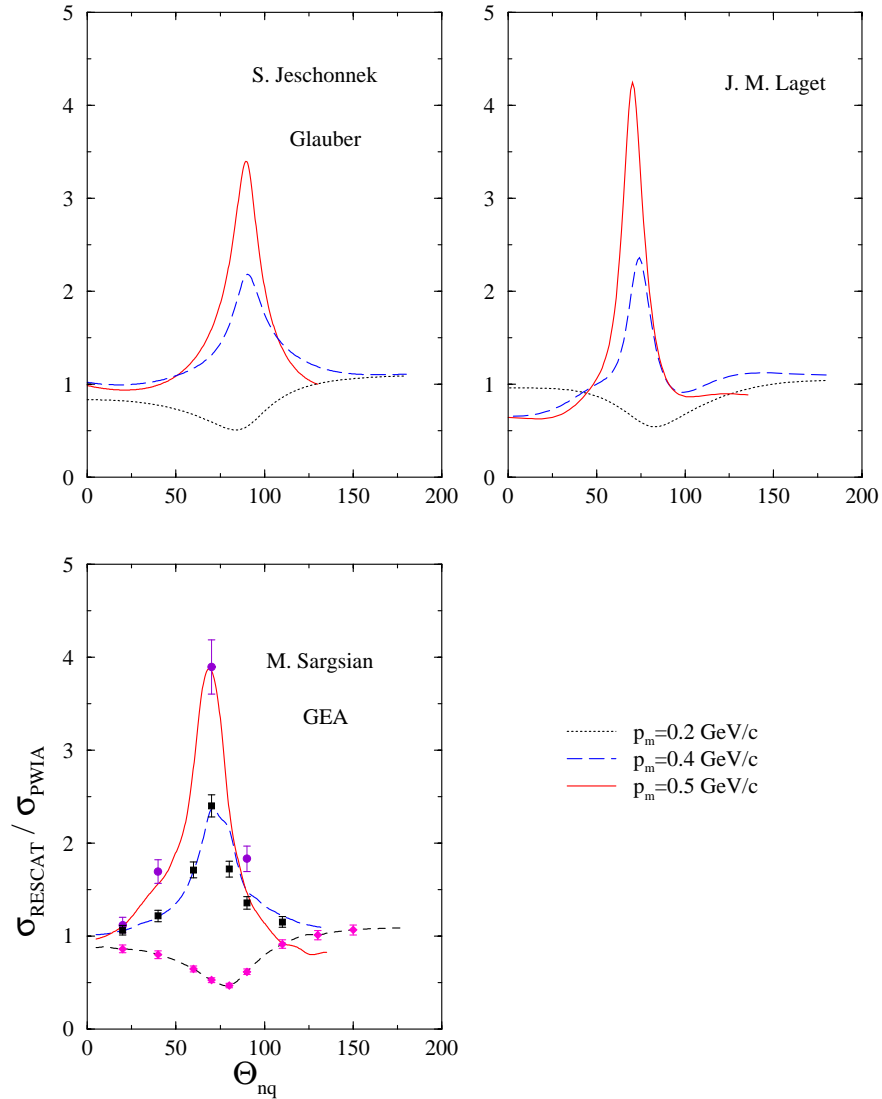


Figure 9: The ratio between the  $D(e,e'p)n$  cross section calculated including FSI and PWIA for  $Q^2 = 4 \text{ (GeV/c)}^2$ . The Calculations are by S. Jeschonnek, J.M. Laget, and M. Sargsian. The points with error bars indicate the projected experimental data.

of 7.5 %. This will reduce the necessary beam time considerably and still provide an excellent measurement.

The detailed kinematics can be found in Tab. 1, 2, 3, 4, 5, 6, 7, 8 and 9. At  $Q^2 = 4 \text{ (GeV/c)}^2$  the hadron and the electron arm will have to be interchanged in order to allow the measurement of the high proton momenta for the large recoil angles. The detector systems however will not have to be interchanged since both spectrometers have a gas Cherenkov detector.

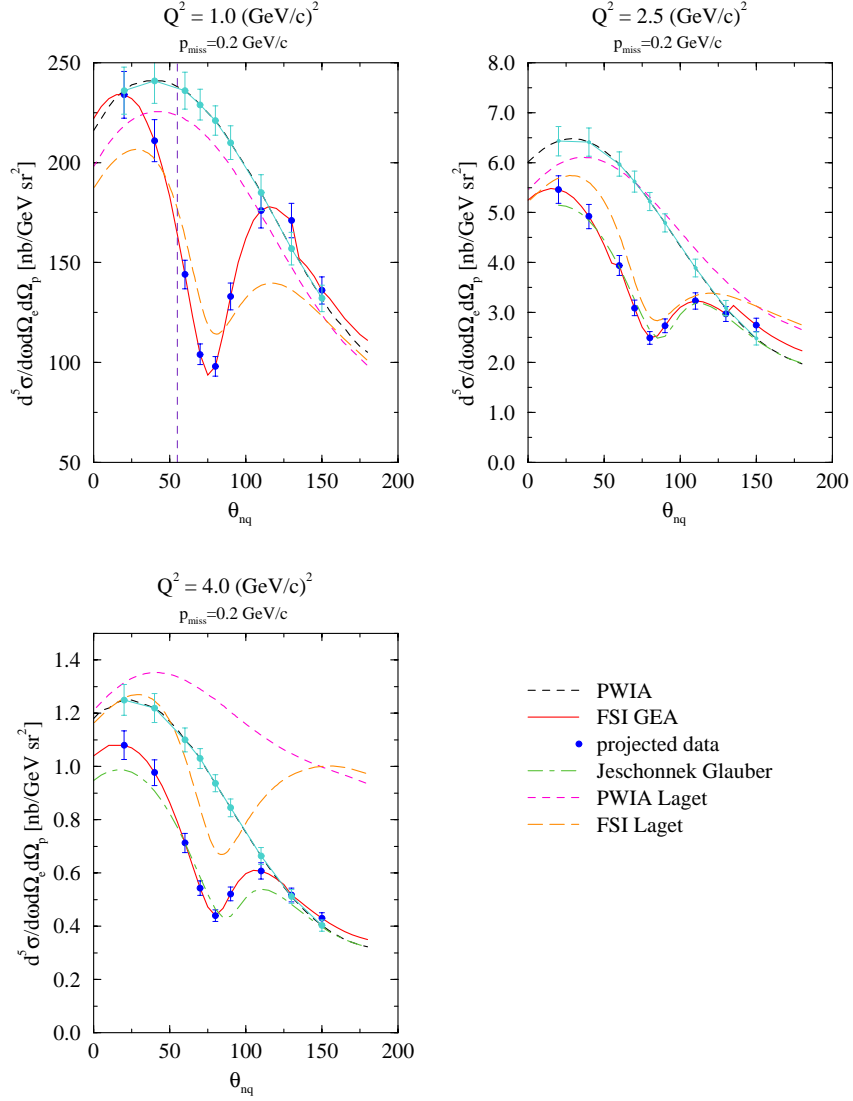


Figure 10: The  $D(e,e'p)n$  cross section for  $p_{miss} = 0.2$  GeV/c as a function of the recoil angle ( $\theta_{nq}$ ) and for various  $Q^2$  values. Note that for small neutron angles and at  $Q^2 = 1.0$  (GeV/c)<sup>2</sup> the eikonal approximation breaks down. (i.e. curves left of the dashed vertical line illustrate this point)

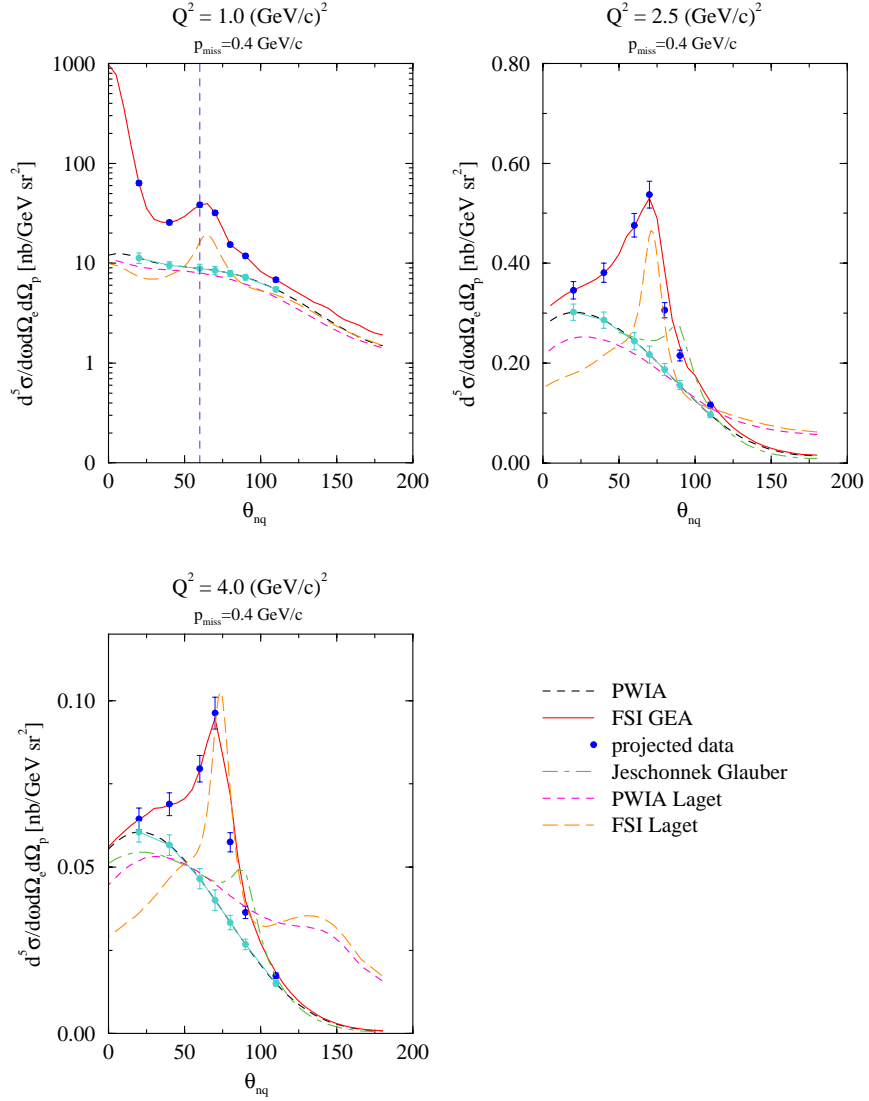


Figure 11: The  $D(e,e'p)n$  cross section for  $p_{miss} = 0.4$  GeV/c as a function of the recoil angle ( $\theta_{nq}$ ) and for various  $Q^2$  values. Note that for small neutron angles and at  $Q^2 = 1.0$  (GeV/c)<sup>2</sup> the eikonal approximation breaks down. (i.e. curves left of the dashed vertical line illustrate this point)

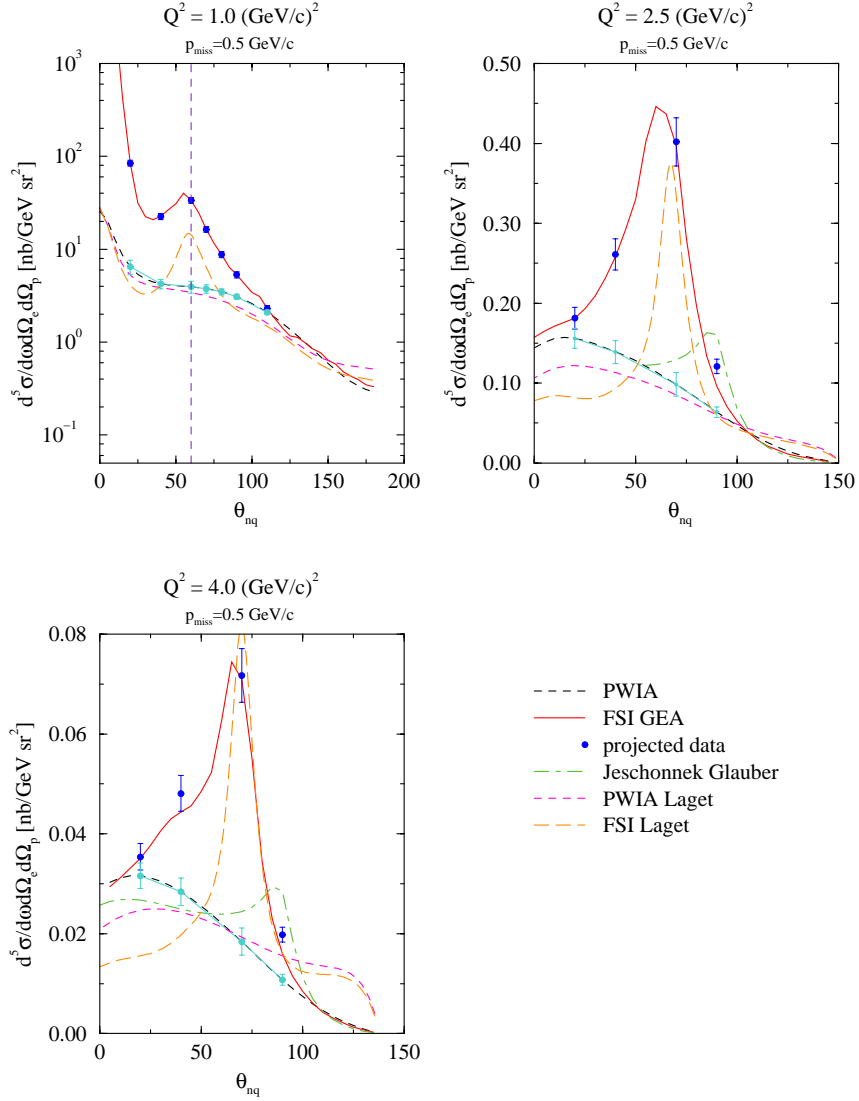


Figure 12: The  $D(e,e'p)n$  cross section for  $p_{miss} = 0.5$  GeV/c as a function of the recoil angle ( $\theta_{nq}$ ) and for various  $Q^2$  values. Note that for small neutron angles and at  $Q^2 = 1.0$  (GeV/c)<sup>2</sup> the eikonal approximation breaks down. (i.e. curves left of the dashed vertical line illustrate this point)

$\theta_{nq}$	$E_f$	$\theta_e$	$P_p$	$\theta_p$
20	3.95	13.91	0.88	67.21
40	3.91	13.98	0.94	68.74
60	3.85	14.09	1.02	67.71
70	3.81	14.16	1.07	66.33
80	3.77	14.23	1.12	64.48
90	3.73	14.31	1.18	62.25
110	3.64	14.49	1.29	57.12
130	3.55	14.67	1.4	51.75
150	3.48	14.82	1.48	46.87

Table 1: Kinematics for  $E_{inc} = 4.32$  GeV/c,  $Q^2 = 1.0$  (GeV/c)<sup>2</sup>,  $p_{miss} = 0.2$  GeV/c

$\theta_{nq}$	$E_f$	$\theta_e$	$P_p$	$\theta_p$
20	3.30	24.19	1.70	48.09
40	3.23	24.44	1.77	48.25
60	3.13	24.85	1.89	46.76
70	3.06	25.12	1.96	45.46
80	2.99	25.43	2.04	43.86
90	2.91	25.77	2.13	42.02
110	2.74	26.56	2.31	37.94
130	2.58	27.41	2.49	33.82
150	2.44	28.16	2.63	30.23

Table 2: Kinematics for  $E_{inc} = 4.32$  GeV/c,  $Q^2 = 2.5$  (GeV/c)<sup>2</sup>,  $p_{miss} = 0.2$  GeV/c

$\theta_{nq}$	$E_f$	$\theta_e$	$P_p$	$\theta_p$
20	3.71	25.83	2.43	39.66
40	3.62	26.15	2.53	39.44
60	3.47	26.70	2.68	37.88
70	3.38	27.07	2.78	36.66
80	3.28	27.49	2.89	35.20
90	3.17	27.98	3.00	33.56
110	2.93	29.11	3.25	29.99
130	2.70	30.39	3.50	26.44
150	2.50	31.57	3.70	23.40

Table 3: Kinematics for  $E_{inc} = 5.4$  GeV/c,  $Q^2 = 4.0$  (GeV/c)<sup>2</sup>,  $p_{miss} = 0.2$  GeV/c

$\theta_{nq}$	$E_f$	$\theta_e$	$P_p$	$\theta_p$
20	4.01	13.79	0.68	77.72
40	3.94	13.93	0.81	80.85
60	3.82	14.15	0.98	77.00
70	3.74	14.29	1.09	73.16
80	3.65	14.47	1.20	68.45
90	3.55	14.66	1.32	63.16
110	3.33	15.16	1.59	51.81

Table 4: Kinematics for  $E_{inc} = 4.32$  GeV/c,  $Q^2 = 1.0$  (GeV/c)<sup>2</sup>,  $p_{miss} = 0.4$  GeV/c

$\theta_{nq}$	$E_f$	$\theta_e$	$P_p$	$\theta_p$
20	3.47	23.58	1.43	55.99
40	3.34	24.02	1.57	56.43
60	3.14	24.80	1.81	52.85
70	3.00	25.35	1.96	49.80
80	2.85	26.04	2.13	46.12
90	2.68	26.89	2.32	41.98
110	2.26	29.31	2.76	33.04

Table 5: Kinematics for  $E_{inc} = 4.32$  GeV/c,  $Q^2 = 2.5$  (GeV/c)<sup>2</sup>,  $p_{miss} = 0.4$  GeV/c

$\theta_{nq}$	$E_f$	$\theta_e$	$P_p$	$\theta_p$
20	3.96	24.97	2.09	46.51
40	3.80	25.52	2.27	46.15
60	3.52	26.52	2.57	42.69
70	3.34	27.25	2.76	39.96
80	3.12	28.18	2.99	36.72
90	2.88	29.39	3.24	33.11
110	2.29	33.08	3.86	25.28

Table 6: Kinematics for  $E_{inc} = 5.4$  GeV/c,  $Q^2 = 4.0$  (GeV/c)<sup>2</sup>,  $p_{miss} = 0.4$  GeV/c

$\theta_{nq}$	$E_f$	$\theta_e$	$P_p$	$\theta_p$
20	4.02	13.79	0.60	82.98
40	3.92	13.96	0.76	86.30
60	3.77	14.24	0.99	79.95
70	3.66	14.44	1.13	74.48
80	3.55	14.68	1.28	68.06
90	3.41	14.96	1.44	61.06
110	3.08	15.77	1.83	46.48

Table 7: Kinematics for  $E_{inc} = 4.32 \text{ GeV}/c, Q^2 = 1.0 \text{ (GeV}/c)^2, p_{miss} = 0.5 \text{ GeV}/c$

$\theta_{nq}$	$E_f$	$\theta_e$	$P_p$	$\theta_p$
20	3.52	23.41	1.32	59.41
40	3.36	23.95	1.50	59.91
70	2.93	25.67	1.99	50.79
90	2.49	27.91	2.47	40.44

Table 8: Kinematics for  $E_{inc} = 4.32 \text{ GeV}/c, Q^2 = 2.5 \text{ (GeV}/c)^2, p_{miss} = 0.5 \text{ GeV}/c$

$\theta_{nq}$	$E_f$	$\theta_e$	$P_p$	$\theta_p$
20	4.04	24.71	1.95	49.41
40	3.84	25.37	2.18	48.95
70	3.26	27.57	2.80	40.70
90	2.64	30.69	3.44	31.70

Table 9: Kinematics for  $E_{inc} = 5.4 \text{ GeV}/c, Q^2 = 4.0 \text{ (GeV}/c)^2, p_{miss} = 0.5 \text{ GeV}/c$

## 5 Count-Rates

The coincidence count-rates have been estimated using the Hall-A monte-carlo program MCEEP [36]. We have used a momentum acceptance of  $\pm 4.5\%$  and an angular acceptance of  $\Delta\phi = \pm 30 \text{ mr}$  and  $\Delta\theta = \pm 65 \text{ mr}$ . Cuts in the recoil angle, and the missing momentum have been defined as mentioned above. No cuts have been applied to  $Q^2$ . A 15 cm liquid deuterium target and a current of  $100\mu\text{A}$  have been assumed, which results in a luminosity of  $L = 4.7 \cdot 10^{38} \text{ cm}^2 \cdot \text{sec}^{-1}$ . The results of these estimates are shown in Tab. 10, 11 and 12.

Singles rates have been estimated using the programs QFS and EPC and have been averaged over the acceptances. The accidental rates (Tab. 13) in a missing mass range from -5 MeV to 10 MeV have been estimated using a coincidence time window of 5 ns and a phase space volume, calculated using MCEEP. For accidental events one can define an effective cross section as follows:

$$\sigma_{acc} = L\tau\sigma_{ep}\sigma_{ee}$$

where  $\tau$  is the coincidence time,  $L$  is the luminosity and  $\sigma_{ep}$  and  $\sigma_{ee}$  are the inclusive proton and electron cross sections respectively. The *accidentals* cross section is a six-fold differential cross section in the electron and proton solid angles and the electron and proton momenta.

$\theta_{nq}$	$Q^2 = 1.0 \text{ (GeV/c)}^2$	$Q^2 = 2.5 \text{ (GeV/c)}^2$	$Q^2 = 4.0 \text{ (GeV/c)}^2$
20	3800	740	124
40	4000	840	175
60	6000	960	120
70	4780	870	150
80	5800	670	180
90	11600	830	155
110	12800	1320	200
130	30500	1200	170
150	27000	1070	120

Table 10: Counts per hour and bin for  $p_{miss} = 0.2 \text{ GeV/c}$ .

$\theta_{nq}$	$Q^2 = 1.0 \text{ (GeV/c)}^2$	$Q^2 = 2.5 \text{ (GeV/c)}^2$	$Q^2 = 4.0 \text{ (GeV/c)}^2$
20	360	68	15
40	530	110	24
60	810	200	36
70	1130	280	52
80	2680	190	36
90	3000	150	24
110	3230	96	11

Table 11: Counts per hour and bin for  $p_{miss} = 0.4 \text{ GeV/c}$ .

$\theta_{nq}$	$Q^2 = 1.0 \text{ (GeV/c)}^2$	$Q^2 = 2.5 \text{ (GeV/c)}^2$	$Q^2 = 4.0 \text{ (GeV/c)}^2$
20	130	37	9
40	390	86	17
60	1260		
70	1330	250	45
80	1150		
90	1590	96	15
110	1860		

Table 12: Counts per hour and bin for  $p_{miss} = 0.5 \text{ GeV/c}$ .

$p_{miss}$ (GeV/c)	$\theta_{ng}$	$Q^2 = 1.0$	$Q^2 = 2.5$	$Q^2 = 4.0$
0.2	40	8	0.01	$4 \cdot 10^{-4}$
0.2	70	192	0.2	$5 \cdot 10^{-3}$
0.2	110	16	0.12	$1.1 \cdot 10^{-2}$
0.4	40	9	$4 \cdot 10^{-3}$	$3 \cdot 10^{-5}$
0.4	70	40	0.4	$1.6 \cdot 10^{-2}$
0.4	110	30	0.3	$4 \cdot 10^{-2}$
0.5	40	142	$5 \cdot 10^{-3}$	
0.5	70	73	0.5	
0.5	100	31	0.4	

Table 13: Accidental counts per hour and bin estimated using QFS and EPC. The signal to noise ratio for all settings is above 10 with the exception of  $p_{miss} = 0.5$  GeV/c and  $\theta_{ng} = 40^\circ$  where it is around 3. This setting is quite close to the deuteron threshold and QFS is not expected to be valid. (all  $Q^2$  in (GeV/c)<sup>2</sup>)

Proton and electron singles rates are well within the capabilities of the spectrometer detector systems. The resulting signal to noise ratio is generally large and we do not anticipate any background problems.

The Pion rates are generally well below the singles rates for electron and protons. In the electron arm, pions will be rejected with the Cherenkov detector. For the majority of kinematic settings pions in the hadron arm can be rejected using time-of-flight measurements since the momenta involved are below 3.5 GeV/c and the corresponding time-of-flight difference between pions and protons is  $\geq 2.9$  ns. Above 3.5 GeV/c an aerogel Cherenkov detector will be used.

## 6 Beam Time Request

We plan to measure a total of 63 different kinematical settings. Table 14 shows the summary of the requested beam time. The beam time on target required to achieve the necessary statistics includes the following items:

- Time to check the spectrometer pointing.
- Time for target changes.
- Measurements on the dummy target cell.
- Time for field changes.
- 4 hours for elastic scattering at each values of  $Q^2$  .
- A factor of 1.3 has been applied to account for radiative losses.

The time allocations for the various items above are from experience gained in the experiments E89-044 and E97-111 when all systems were working smoothly. We have not included

time for changes of the spectrometer polarity since this depends on the run plan. Also no efficiency factor for Hall A has been taken into account.

$Q^2$ (GeV/c) <sup>2</sup>	$p_{miss}$ (GeV/c)	Data Taking	Overhead	Subtotal
1.0	0.2	5.9	21.3	27.2
	0.4	7.7	15.9	23.6
	0.5	8.1	17.8	25.9
2.5	0.2	5.8	21.3	27.1
	0.4	28.6	13.9	42.5
	0.5	12.2	8.2	20.4
4.0	0.2	31.3	21.3	52.6
	0.4	164.3	13.9	178.2
	0.5	60.6	8.2	68.8
Optics Commissioning				16
Target Commissioning				16
TOTAL				498.3

Table 14: Beam Time Overview

## References

- [1] L.C. Alexa *et al.*, Phys. Rev. Lett. **82** (1999) 1374.
- [2] W. Van Orden, *The Deuteron in the Light of the New Data from JLab*, Plenary talk at the Jefferson Lab User Meeting, 24-25 June 1999.
- [3] S. Rock *et al.*, Phys. Rev. **D46** (1992) 24; P. Bosted, R.G. Arnold, S. Rock and Z.M. Szalata, Phys. Rev. Lett. **49** (1982) 1380.
- [4] O. Benhar, A. Fabrocini, S. Fantoni, G.A. Miller, V.R. Pandharipande, and I. Sick, Phys. Rev. **C44** (1991) 2328.
- [5] O. Benhar, A. Fabrocini, S. Fantoni, V.R. Pandharipande, and I. Sick, Phys. Rev. **C5** (1994).
- [6] L.L. Frankfurt, M.I. Strikman, D.B. Day and M.M. Sargsian, Phys. Rev. **C48** (1993) 2451.
- [7] A. Bussiere *et al.*, Nucl. Phys. **A365** (1981) 349. %
- [8] K.I. Blomqvist *et al.*, Phys. Lett. **B429** (1998) 33.
- [9] R.J. Glauber, Phys. Rev. **100** (1955) 242.
- [10] L.L. Frankfurt, W.G. Greenberg, J.A. Miller, M.M. Sargsian and M.I. Strikman, Z. Phys. **A352** (1995) 97.
- [11] L.L. Frankfurt, M.M. Sargsian and M.I. Strikman, Phys. Rev. **C56** (1997) 1124.
- [12] T.G. O'Neill *et al.*, Phys. Lett. **B351** (1995) 87.
- [13] D. Abbott *et al.*, Phys. Rev. Lett. **80** (1998) 5072.
- [14] H. Arenhovel, W. Leidemann and E.L. Tomusiak, Phys. ReV. **C46** (1992) 455.
- [15] J.-M. Laget, in *Modern Topics in Electron Scattering*, Ed. by B. Frois and I. Sick (World Scientific, 1991) 290, and references therein.
- [16] J.-M. Laget, Nucl. Phys. **A579** (1994) 333.
- [17] E. Voutier, V. Breton, J.-M. Laget, C. Marchand, J. Marroncle, J.-F. Mathiot, A. Pastor and Th. Russew, Proceedings of the ELFE Workshop on Hadronic Physics, Ed. by N. d'Hose *et al.* (St-Malo, 1996) 107;  
J.-M. Laget, Proceedings of the Workshop on Color Transparency (<http://isnwww.in2p3.fr/ct97>), Ed. E. Voutier (Grenoble, 1997) 131.
- [18] J.-M. Laget, Physics and Instrumentation with 6-12 GeV Beams, Ed. by S. Dytman *et al.* (Newport News, 1998), p.57.

- [19] A. Bianconi, S. Jeschonnek, N.N. Nikolaev and B.G. Zakharov, Phys. Lett. **B343** (1995) 13.
- [20] S. Jeschonnek, **nucl-th/0009086** (2000).
- [21] D.O. Riska, Phys. Rep. **181** (1989) 207.
- [22] J. Speth and A.W. Thomas, Adv. Nucl. Phys. **24** (1997) 83.
- [23] H. Arenhovel, in *Modern Topics in Electron Scattering*, Ed. by B. Frois and I. Sick (World Scientific, 1991) 136.
- [24] L.L. Frankfurt, G.A. Miller, M.M. Sargsian and M.I. Strikman, Phys. Rev. Lett. **84** (2000) 3045.
- [25] L.L. Frankfurt and M.I. Strikman, Phys. Rep. **76**, (1981) 215; Phys. Rep. **160**, (1988).
- [26] F. Gross, Phys. Rev. **C26** (1982) 2203.
- [27] B.D. Keister and W.N. Polyzou, in *Advances in Nuclear Physics*, Ed. J.W. Negele and E. Voght, **V.20** (1991) 225.
- [28] L.A. Kondratyuk, J. Vogelzang and M.S. Franchesko, Phys. Lett. **B98** (1981) 405.
- [29] J. Carbonell, B. Desplanques, V.A. Karmanov and J.-F. Mathiot, Phys. Rep. **300** (1998) 215.
- [30] T.J. de Forest, Nucl. Phys. **A392** (1983) 232.
- [31] J.J. Aubert *et al.*, Phys. Lett. **B123** (1983) 275;  
A. Bodek *et al.*, Phys. Rev. Lett. **50** (1983) 1431; Phys. Rev. Lett. **51** (1983) 534.
- [32] L.L. Frankfurt and M.I. Strikman, Nucl. Phys. **B250** (1985) 143.
- [33] M.R. Frank, B.K. Jennings, G.A. Miller, Phys. Rev. **C54** (1996) 920.
- [34] L.L. Frankfurt and M.I. Strikman, Phys. Rep. **160** (1988) 235.
- [35] J.-E. Ducret *et al.*, Phys. Rev. **C49** (1994) 1783.
- [36] P. E. Ulmer, Computer Program MCEEP, *Monte Carlo for ee'p Experiments*, CEBAF Technical Note No. 91-101, 1991.

## A Relation to Experiment E94-004

The goal of experiment E94-004 is to determine the individual response functions  $R_L$ ,  $R_T$  and  $R_{LT}$  of the D(e,e'p)n reaction in quasi free kinematics ( $x = 1$ ). One set of measurements aims at determining the  $R_{LT}$  response function for  $Q^2 = 0.81$  (GeV/c)<sup>2</sup> and for recoil momenta up to 0.5 GeV/c. A set of data at  $Q^2 = 2.1$  (GeV/c)<sup>2</sup> will be used to determine  $R_{LT}$  for  $p_{miss}$  values of 0.1, 0.2 and 0.3 GeV/c. In addition the  $Q^2$  dependence of the  $R_L$  and the  $R_T$  response function at  $p_{miss} = 0$  (GeV/c) will be determined.

The proposed experiment differs from this experiment in the following main points:

- We are NOT proposing to determine individual response functions.
- The goal of the proposed experiment is to measure the D(e,e'p)n cross section at *constant*  $p_{miss}$  and  $Q^2$  values but at various angles of the recoiling nucleon with respect to  $\vec{q}$ .
- We want to determine the  $Q^2$  -dependence of these angular distributions between  $Q^2 = 1$  (GeV/c)<sup>2</sup> and  $Q^2 = 4$ . (GeV/c)<sup>2</sup>.
- The selection of the  $p_{miss}$  values in the proposed experiment has been driven by the expected rescattering behavior in the np system. It is therefore crucial that these  $p_{miss}$  values are measured.

The data expected from experiment E94-004 at  $Q^2 = 0.8$  (GeV/c)<sup>2</sup> could only provide *one* point in the angular distribution at low  $Q^2$  for  $p_{miss} = 0.2, 0.4$  and 0.5 GeV/c and at  $Q^2 = 2$ . (GeV/c)<sup>2</sup> *one* point in the angular distribution for  $p_{miss} = 0.2$  GeV/c.

## B Relation to Experiment E94-102

This experiment studies the  $d(e, e'p)X$  reaction, detecting the recoiling proton. The range in  $x$  studied lies between  $x = 1$  and  $x = 0.2$ . The focus of this experiment is inelastic scattering off the neutron. Due to statistical limitations, this experiment does not allow the fine binning in the relevant kinematical variables as proposed in this experiment. In contrast the proposed experiment will provide valuable data for the interpretation of the experimental results of E94-102.

## C Relation to Experiment E94-019

This experiment measures the  $e, e'p$  reaction on a series of nuclei including the deuteron using CLAS. The focus of this experiment is to determine the  $Q^2$  dependence of the nuclear transparency using rescattering. Due to statistical limitations, this experiment does not measure angular distributions. The proposed experiment will provide complementary data which will form a baseline for a clear interpretation of the transparency phenomenon – the subject of E94-019.